Title

R-loop formation at Snord116 mediates topotecan inhibition of Ube3a-antisense and allele-specific chromatin decondensation

Journal

Proceedings of the National Academy of Sciences of the United States of America, 110(34)

ISSN

0027-8424

Authors

Powell, Weston T
Coulson, Rochelle L
Gonzales, Michael L
et al.

Publication Date

2013-08-20

DOI

10.1073/pnas.1305426110

Peer reviewed

R-loop formation at *Snord116* mediates topotecan inhibition of *Ube3a-antisense* and allele-specific chromatin decondensation

Weston T. Powell[a], Rochelle L. Coulson[a], Michael L. Gonzales[a], Florence K. Crary[a], Spencer S. Wong[a], Sarrita Adams[a], Robert A. Ach[b], Peter Tsang[b], Nazumi Alice Yamada[b], Dag H. Yasui[a], Frédéric Chédin[c], and Janine M. LaSalle[a,1]

[a]Medical Microbiology and Immunology, Genome Center, Medical Investigation of Neurodevelopmental Disorders (MIND) Institute, and [c]Department of Molecular and Cellular Biology, University of California, Davis, CA 95616; and [b]Agilent Laboratories, Agilent Technologies, Santa Clara, CA 95051

Edited by Mark Groudine, Fred Hutchinson Cancer Research Center, Seattle, WA, and approved July 9, 2013 (received for review March 20, 2013)

Prader–Willi syndrome (PWS) and Angelman syndrome (AS) are oppositely imprinted autism-spectrum disorders with known genetic bases, but complex epigenetic mechanisms underlie their pathogenesis. The PWS/AS locus on 15q11–q13 is regulated by an imprinting control region that is maternally methylated and silenced. The PWS imprinting control region is the promoter for a one megabase paternal transcript encoding the ubiquitous protein-coding *Snrpn* gene and multiple neuron-specific noncoding RNAs, including the PWS-related *Snord116* repetitive locus of small nucleolar RNAs and host genes, and the antisense transcript to AS-causing ubiquitin ligase encoding *Ube3a* (*Ube3a-ATS*). Neuron-specific transcriptional progression through *Ube3a-ATS* correlates with paternal *Ube3a* silencing and chromatin decondensation. Interestingly, topoisomerase inhibitors, including topotecan, were recently identified in an unbiased drug screen for compounds that could reverse the silent paternal allele of *Ube3a* in neurons, but the mechanism of topotecan action on the PWS/AS locus is unknown. Here, we demonstrate that topotecan treatment stabilizes the formation of RNA:DNA hybrids (R loops) at G-skewed repeat elements within paternal *Snord116,* corresponding to increased chromatin decondensation and inhibition of *Ube3a-ATS* expression. Neural precursor cells from paternal *Snord116* deletion mice exhibit increased *Ube3a-ATS* levels in differentiated neurons and show a reduced effect of topotecan compared with wild-type neurons. These results demonstrate that the AS candidate drug topotecan acts predominantly through stabilizing R loops and chromatin decondensation at the paternally expressed PWS *Snord116* locus. Our study holds promise for targeted therapies to the *Snord116* locus for both AS and PWS.

neurodevelopment | brain | HBII85 | MBII85 | snoRNA

Prader–Willi syndrome (PWS) and Angelman syndrome (AS) are imprinted neurodevelopmental disorders caused by oppositely inherited deficiencies of chromosome 15q11–q13. AS and PWS are both characterized by hypotonia at birth, disordered sleep, autistic features, and intellectual disabilities, but the diseases differentiate into phenotypically distinct syndromes in early childhood (1, 2). Seizures, ataxia, and inappropriate laughter characterize AS, whereas hyperphagia leading to obesity and obsessive-compulsive behaviors characterize PWS. Maternal mutations in *UBE3A*/*Ube3a* in humans and mice have identified the loss of function of this ubiquitin E3 ligase encoding gene as the cause of AS (3, 4). For PWS, small deletions of the *HBII-85*/*SNORD116* locus (5–7) and two mouse models of *Snord116* deletions (8, 9) have identified the minimal causative deficiency to be the paternally expressed, highly repetitive, long noncoding RNA (lncRNA) that is processed into multiple small nucleolar RNAs (snoRNAs) and spliced nuclear retained host genes (*116HG* and *115HG*) (10, 11).

A recent drug screen discovered that topoisomerase inhibitors, including topotecan, reduce *Ube3a-ATS* by an unknown mechanism to reverse the silencing of paternal *Ube3a* in mouse neurons and brain (12). Topotecan activates paternal *Ube3a* by reducing the abundance of an antisense transcript, *Ube3a-ATS*, at the 3′ end of a 1-Mb paternal transcript originating at the PWS imprinting control region (PWS-ICR; Fig. 1*A*) (13). *Ube3a-ATS* is an atypical RNA polymerase II transcript that is not polyadenylated and silences paternal *Ube3a* in a transcription-dependent manner, most likely by transcription through the locus (14). Such a mechanism of imprinted transcriptional silencing from an antisense lncRNA has also been observed at the imprinted *Airn* antisense to the growth factor receptor encoding *Igf2r* (15). *Ube3a-ATS* is expressed only in neurons, although transcription initiating at the PWS-ICR occurs in all tissues to give rise to ubiquitously expressed *Snrpn*. Regulation of *Ube3a-ATS* appears to occur through alternative transcription termination potentially related to transcription initiating at upstream U-exons, although the mechanism has not been identified (16, 17). In nonneuronal cells, transcription terminates within the *Snord116* region, but in neurons, transcription continues through the *Snord116* region to generate *Ube3a-ATS* and silence paternal *Ube3a* (14). Reversing paternal *UBE3A* silencing with topotecan holds promise as a therapy for AS because it would compensate for loss of maternal *UBE3A*; however, concerns about specificity persist (18).

Topotecan acts as an inhibitor of topoisomerase I (19), but the mechanism by which it specifically represses *Ube3a-ATS* is unknown. Topoisomerase activity is necessary to relieve the topological strain caused by transcription (20). Loss of topoisomerase activity in front of the elongating RNA polymerase leads to increased supercoiling and inhibition of transcription (21), whereas loss of topoisomerase activity behind the RNA polymerase complex leads to melting of the DNA and the formation of DNA:RNA hybrids called R loops (22). R loops form at CpG island promoters, the 3′ ends of genes, and recombination sites (23–25). The formation of R loops slows RNA polymerase by increasing the forces impeding transcriptional progression including steric hindrance caused by wrapping of the RNA (26, 27).

Here we demonstrate that R-loop formation occurs over repetitive intronic segments of high GC skew in mouse *Snord116* and human *SNORD116* PWS loci and that this genetic locus mediates the effects of topotecan treatment on *Ube3a-ATS* expression. Topetecan increased formation of R loops and chromatin decondensation over the active paternal *Snord116* allele and stalled transcriptional progression through *Ube3a-ATS*. These results improve understanding of the relationship between imprinting, chromatin dynamics, and transcriptional regulation of the imprinted PWS/AS locus that will inform more targeted therapies for these and other related autism-spectrum disorders.

Author contributions: W.T.P., M.L.G., F.C., and J.M.L. designed research; W.T.P., R.L.C., M.L.G., F.K.C., S.S.W., and D.H.Y. performed research; M.L.G., S.A., R.A.A., P.T., N.A.Y., D.H.Y., and F.C. contributed new reagents/analytic tools; W.T.P., R.L.C., and F.C. analyzed data; and W.T.P. and J.M.L. wrote the paper.

Conflict of interest statement: R.A.A., P.T., and N.A.Y. are employees of Agilent, Inc.

This article is a PNAS Direct Submission.

Freely available online through the PNAS open access option.

[1]To whom correspondence should be addressed. E-mail: jmlasalle@ucdavis.edu.

This article contains supporting information online at www.pnas.org/lookup/suppl/doi:10.1073/pnas.1305426110/-/DCSupplemental.

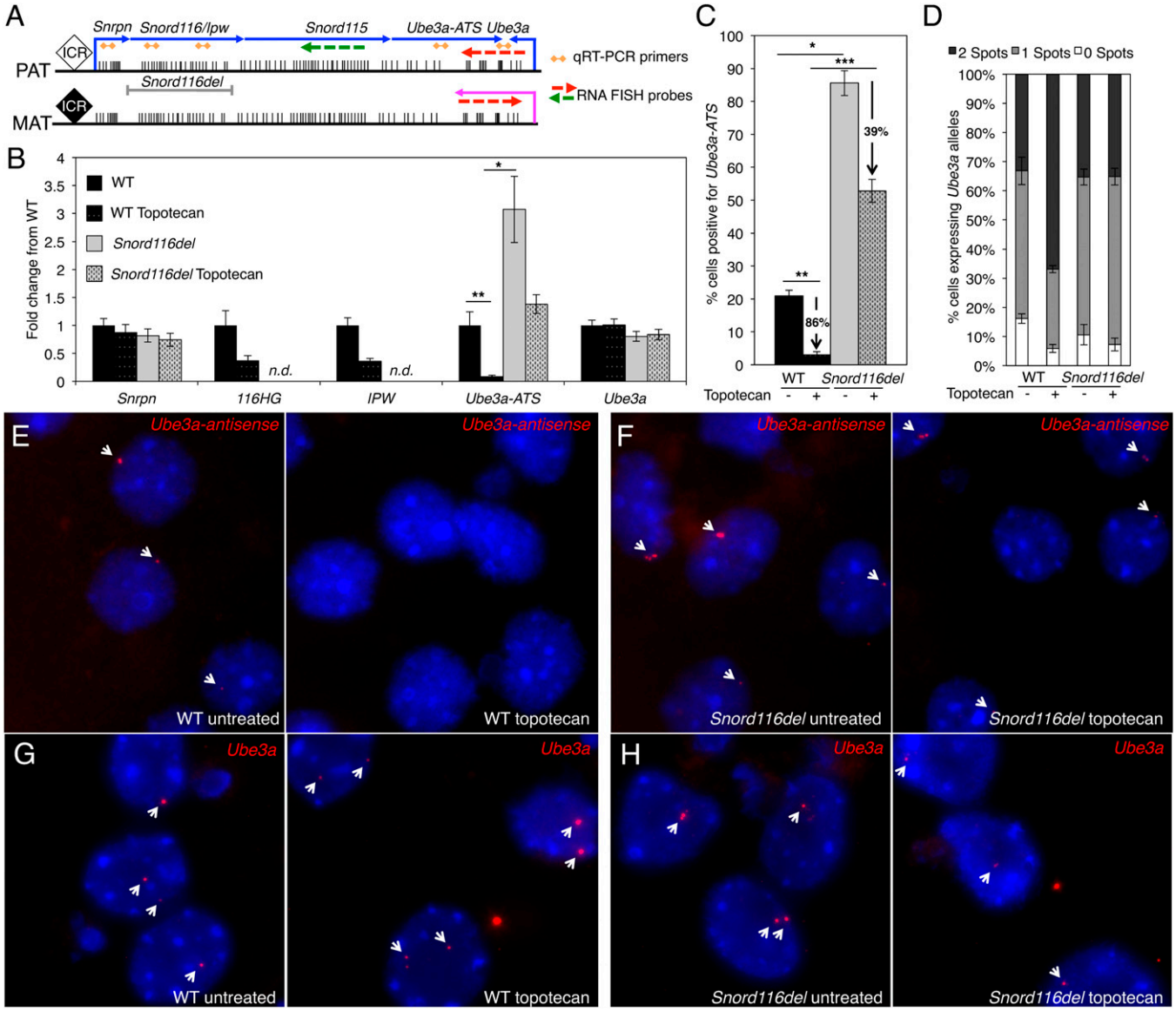

Fig. 1. Deletion of the *Snord116* locus mitigates topotecan mediated inhibition of *Ube3a-ATS*. (*A*) Schematic of *Snrpn* to *Ube3a* with genes, primer locations, RNA FISH probe locations, and location of deletion in *Snord116del* mouse. Paternal and maternal alleles indicated by Pat and Mat, respectively. (*B*) qRT-PCR of RNA isolated from 10 d in vitro cultured neurons normalized to *Gapdh* and graphed relative to WT mock treated levels. (*C*) Percentage of nuclei positive for *Ube3a-ATS* RNA FISH on 10 d in vitro cultured neurons from WT and *Snord116del* mice mock treated or treated with 300 nM topotecan. % reduction labeled, and graphed in Fig. S1. (*D*) Results for RNA FISH using the *Ube3a* sense probe graphed as % nuclei exhibiting biallelic (two spots), monoallelic (one spot), or nonexpressing (no spots) pattern of *Ube3a* Representative images of *Ube3a-ATS* (*E* and *F*) or *Ube3a* (*G* and *H*) RNA FISH in WT neurons (*Left*) or *Snord116del* neurons (*Right*) treated with or without 300 nM topotecan. White arrows indicate RNA FISH signals (red). Nuclei stained with DAPI (blue). Results are graphed as mean ± SEM from four biological replicates of 150–200 nuclei each. $*P < 0.05$, $**P < 0.01$, $***P < 0.001$. n.d., not detectable.

Results

To determine the genetic requirement for the *Snord116* PWS locus in mediating topotecan action, neural precursor cell (NPC) cultures from mice with paternal deletion of *Snord116* (*Snord116del*) and wild-type (WT) littermates were differentiated to neurons and treated with 300 nM topotecan using conditions that effectively activate paternal *Ube3a* in mouse neurons (12). Steady-state transcript levels assayed by quantitative reverse transcriptase PCR (qRT-PCR) demonstrated significantly increased *Ube3a-ATS* transcript levels in *Snord116del* compared with WT neurons, as well as expected deficiencies in host gene transcripts *116HG* and *IPW* with no significant change in *Snrpn* and *Ube3a* transcript levels (9) (Fig. 1*B*). RNA fluorescence in situ hybridization (FISH) using a probe designed to detect *Ube3a-ATS* showed that 80–90% of *Snord116del* neurons expressed *Ube3a-ATS*, compared with only 25% of WT neurons (Fig. 1*C*, *E*, and *F*). Topotecan treatment of neurons derived from WT NPCs resulted in an 86% reduction in the number of cells showing *Ube3a-ATS* signal and an 89% reduction in *Ube3a-ATS* transcript levels, as expected (12) (Fig. 1 *B*, *C*, and *E* and Fig. S1). In contrast, the *Snord116* deletion diminished the inhibitory effect of topotecan treatment on *Ube3a-ATS* expression, with only 39% reduction in the number of *Ube3a-ATS* positive cells, and minimal decrease in *Ube3a-ATS* transcript levels ($P = 0.0546$) (Fig. 1 *B*, *C*, and *F*). No significant change in *Snrpn* transcript levels was observed with topotecan treatment, suggesting that topotecan acts between *Snrpn* and *Ube3a-ATS* within the *Snord116* region (Fig. 1*B*). Although *Ube3a* transcript levels measured by qRT-PCR were unchanged with topotecan treatment, RNA FISH using a *Ube3a* sense-specific probe demonstrated an expected increase in the number

of nuclei showing two *Ube3a* signals (Fig. 1 *D* and *G*), confirming the derepression of the paternal allele shown previously (12). In contrast, there was no associated change in the number of cells expressing *Ube3a* biallelically with *Snord116* deletion (Fig. 1 *D* and *H*). Two-color RNA FISH using probes to detect *115HG* and sense *Ube3a* RNA revealed that the increase in biallelic expression in WT neurons with topotecan treatment coincided with a loss of *115HG* expression, suggesting that RNA polymerase is not progressing beyond the *116HG* locus in cells that reexpress paternal *Ube3a* (11) (Fig. S1). ChIP-qPCR analysis provided supportive evidence that topotecan treatment reduced the progression of RNA Pol-II downstream of *Snord116* (Fig. S2). Together, these results demonstrate that the paternal *Snord116* locus is required for optimal topotecan-driven inhibition of *Ube3a-ATS*. Furthermore, because transcript levels were unaffected at the *Snrpn* 5′ end, these results indicate that topotecan acts primarily within the *Snord116* locus.

We previously demonstrated that the paternal *Snrpn-Ube3a* chromatin becomes decondensed in a transcription-dependent and DNase-sensitive manner in postnatal neurons (28). Because topotecan reduces transcription of *Ube3a-ATS*, we investigated its effect on the chromatin structure of the maternal and paternal alleles by performing DNA FISH for the *Snrpn-Ube3a* locus on WT and *Snord116del* neurons. As previously shown, the paternal allele was decondensed relative to the maternal allele (Fig. 2*A*). Topotecan specifically and significantly increased the decondensation of the paternal allele in WT neurons (Fig. 2 *A* and *C*). In contrast, topotecan did not change the length of the decondensed paternal allele in *Snord116del* neurons (Fig. 2 *A* and *D*). DNA FISH analysis of the *Snord116* locus demonstrated that the increased decondensation with topotecan treatment occurs primarily at *Snord116* (Fig. 2 *B* and *E*). Chromatin decondensation measured by DNA FISH was neuron-specific (Fig. 2 *E* and *F*), corresponding to tissue-specific differences in nucleosome occupancy at *Snord116 in vivo* measured by chromatin immunoprecipitation (ChIP) for total histone H3 (Fig. S2). These results show that *Snord116* is required for topotecan-mediated chromatin decondensation at the *Snrpn-Ube3a* region, and thus that *Snord116* is the specific topotecan-responsive region.

To identify potential sequence characteristics of the *Snord116* region that could explain the specific nature of topotecan activity, we quantified the distribution of G and C bases across the two DNA strands, a property called GC skew (Fig. 3*A*). In both mouse and human, the introns in the *Snord116* repeat region showed positive GC skew on the transcribed strand (Fig. S3). This GC skew pattern is conserved from mouse to human, even though the sequence itself does not show conservation as measured using phyloP or phastCons (Fig. S3). Positive GC skew on the transcribed strand of a GC-rich region is predictive of the potential to form cotranscriptional R loops (Fig. 3*B*) (23). R loops, which are structurally more similar to A-form DNA than to the typical B-form DNA:DNA duplex (29), have been shown to prevent nucleosome binding in vitro (30). In addition, R loops have negative effects on transcription elongation (22, 24, 27), and inhibition of topoisomerase activity has been shown in yeast and human cells to lead to increased R-loop formation (22, 31). Due to the G-richness of the transcribed strand in the *Snord116* repeat region and the stabilizing effect of topoisomerase inhibition on R loops, we hypothesized that increased R-loop formation was responsible for the effects of topotecan on this locus.

To test for R-loop formation at a GC-skewed locus and at *Snord116*, we cloned a control R-loop forming region (mouse *Airn*; ref. 23) in the physiologic (G-rich RNA) or nonphysiologic (C-rich RNA) orientation and intronic *Snord116* repeat regions from mouse and human genomic DNA into in vitro transcription vectors and inducible episomal vectors (Fig. S4). R-loop formation upon in vitro transcription can be detected as an RNase H-sensitive gel-shift of the plasmid from the supercoiled state (Fig. 3*C*, arrowhead) to the relaxed state (Fig. 3*C*, arrow). The presence of R loops can be confirmed by immunoblotting analysis with the S9.6 DNA:RNA-specific antibody (23) (Fig. 3*C*). Similar to the control *Airn* region, cloned genomic regions from mouse *Snord116* and human *SNORD116* exhibited R-loop formation with in vitro transcription by gel-shift analysis and

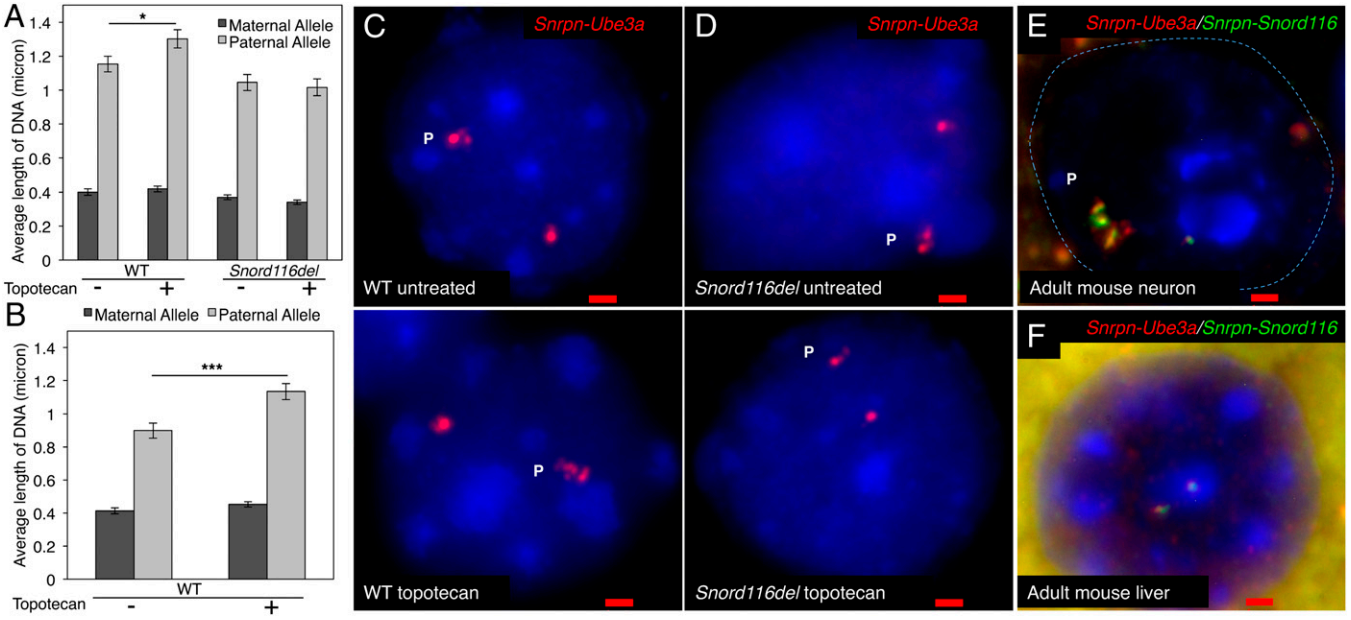

Fig. 2. Topotecan treatment increases chromatin decondensation of the *Snord116* region. (*A*) DNA FISH signal length of the entire *Snrpn-Ube3a* region on paternal (decondensed) and maternal (condensed) alleles in 10 d in vitro cultured neurons from WT and *Snord116del* mice that were treated with or without 300 nM topotecan. (*B*) DNA FISH measurements of shorter *Snrpn-Snord116* region in WT mice, showing topotecan effect on chromatin decondensation at *Snord116*. (*C* and *D*) Representative images of DNA FISH in WT (*C*) or *Snord116del* (*D*) neurons treated without (*Upper*) or with (*Lower*) topotecan. (*E*) Combined DNA FISH of *Snrpn-Ube3a* (red) and *Snrpn-Snord116* (green) in an adult mouse neuron with nucleus outlined showing overlap on paternal decondensed allele of longer and shorter FISH probes. (*F*) Adult mouse liver nucleus using the same combined FISH probes as *E* but the lack of chromatin decondensation. Paternal decondensed allele (P) is shown in each neuronal image. (Scale bar: 1 μm.) Nuclei counterstained by DAPI (blue). Results are graphed as mean ± SEM from two biological replicates. $*P < 0.05$, $**P < 0.01$, $***P < 0.001$.

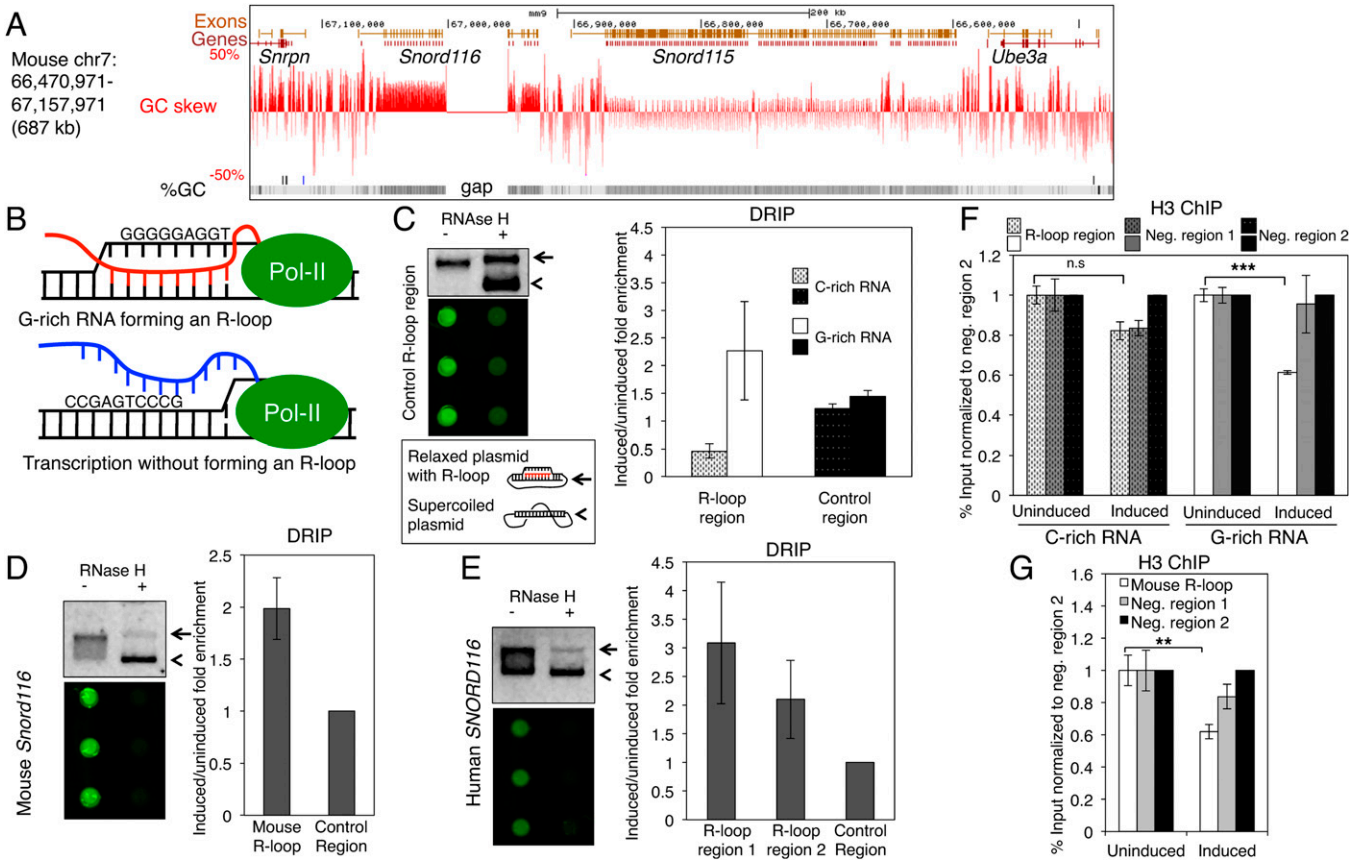

Fig. 3. The mouse *Snord116* region gives rise to a G-rich primary RNA and R-loop formation depletes nucleosomes. (*A*) GC skew (red, +50% to −50%) is mapped over the *Snrpn* to *Ube3a* locus together with exon locations and GC-percent in the UCSC genome browser. (*B*) Diagram showing cotranscriptional R-loop formation with a G-rich sequence (red) but not a C-rich sequence (blue). (*C*) A control R-loop forming region shows decreased plasmid supercoiling upon in vitro transcription that disappears with RNase H treatment (*Upper*) and evidence for R loops by dot blot (*Lower*). DRIP confirms R-loop formation when G-rich RNA is produced, but not C-rich RNA. (*D* and *E*) A cloned G-rich intron from mouse *Snord116* (*D*) and human *SNORD116* (*E*) showed a change in plasmid supercoiling (*Upper*) and R-loop detection by dot blot (*Lower*) when in vitro transcribed, which were diminished by RNase H treatment. DRIP confirms that *Snord116* and *SNORD116* form R loops upon transcription induction in cells. (*F*) A transcribed region shows a decrease in nucleosome occupancy when a G-rich RNA is produced, but not a C-rich RNA. (*G*) Cloned mouse *Snord116* shows a decrease in nucleosome occupancy upon induction of transcription. Results are graphed as mean ± SEM from three replicates (DRIP) or six replicates (ChIP). $*P < 0.05$, $**P < 0.01$, $***P < 0.001$.

immunoblotting (Fig. 3 *D* and *E*). Episomes are stably replicating, chromatinized extrachromosomal DNA entities that can be used to measure R-loop formation by DNA:RNA immunoprecipitation (DRIP) followed by qPCR (DRIP-qPCR) using the S9.6 antibody. Here, R loops were enriched only when transcription was induced through the control *Airn* region in the physiologic (G-rich RNA) orientation (Fig. 3*C*). In contrast, the nonphysiologic (C-rich RNA) orientation did not result in R-loop formation, nor did a constitutively expressed control region (Fig. 3*C*). Episomes carrying regions cloned from mouse *Snord116* and human *SNORD116* also showed R-loop formation by DRIP upon induction of transcription in the physiologic orientation (Fig. 3 *D* and *E*). The presence of a G-skewed sequence was inhibitory to transcription because, under similar culture and induction conditions, a C-skewed sequence induced more readily, compared with a G-skewed sequence and exhibited leaky read-through transcription in the absence of Doxycycline induction (Fig. S4).

Having established that R loops form when transcription was induced on episomes, we performed H3 ChIP to measure the effect that R-loop formation may have on nucleosome occupancy. Coinciding with orientation-specific R-loop formation, H3 ChIP showed a significant decrease in nucleosome occupancy with the induction of transcription only when the transcribed region was in the physiologic orientation (Fig. 3*F*). Confirming that R-loop formation on the *Snord116* intronic sequence leads to loss of nucleosome occupancy, H3 ChIP of the *Snord116* episome showed depletion of nucleosomes relative to a negative control region when transcription was induced (Fig. 3*G*). Together, these results indicate that R-loop formation at *Snord116* can cause transcriptionally dependent chromatin decondensation of this locus.

For further evidence of R-loop formation at *Snord116* in vivo, we performed DRIP-qPCR on genomic DNA isolated from WT adult mouse cerebellum. DRIP-qPCR revealed R-loop formation at the *Snord116* locus and GC skewed positive controls, but not at an unskewed locus (Fig. 4*A*). In addition, combined immunofluorescence with the S9.6 R-loop antibody and DNA FISH to *Snrpn-Ube3a* showed that the two signals colocalized at the decondensed paternal allele (Fig. 4*B* and Fig. S5). In addition, topotecan treatment of neurons resulted in increased R-loop formation detected by DRIP at all loci, but R-loop formation was greater at *Snord116* compared with three control loci (Fig. 4*C*). The combined results of these analyses demonstrate that R loops form under physiologic conditions at *Snord116*, but topotecan stabilizes increased R-loop formation at *Snord116*.

Discussion

Much more is known about the mechanism of transcriptional initiation regulation at the promoters of genes compared with regulation of transcription progression (32), particularly for long transcripts such as *Snrpn-Ube3a*. In this study, we provide evidence for R-loop formation in G-rich repeats of the *Snord116* locus causing displacement of nucleosomes in a transcription-dependent manner corresponding to chromatin decondensation of the paternal allele. Our previous study had shown that transcription on the

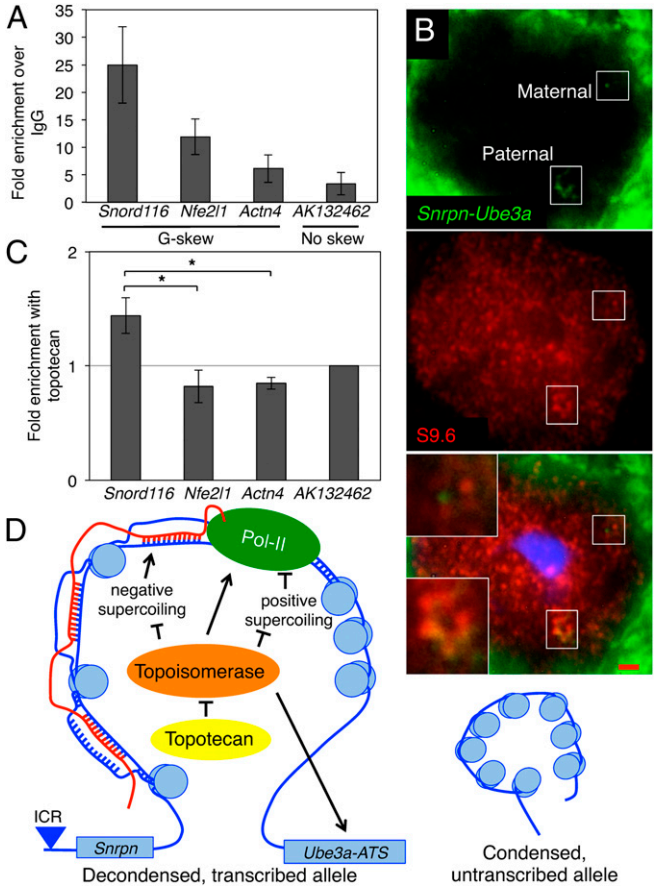

Fig. 4. The endogenous *Snord116* region forms R loops in neurons and topotecan increases R-loop formation at *Snord116*. (*A*) DRIP of cerebellum DNA reveals R-loop formation at *Snord116*, and two positive control loci (*Nfe2l1* and *Actn4*), but not a negative control region (*AK132462*). (*B*) Combined immuno-FISH reveals R-loop formation on the decondensed paternal allele. (Scale bar: 1 μm.) (*C*) DRIP of DNA from topotecan and mock treated neurons shows increased R-loop signal at *Snord116*, but not three other loci. (*D*) A model for topotecan inhibition of topoisomerase I actions leading to stabilization of R-loop formation in *Snord116* leading to chromatin decondensation and mediating topotecan inhibition of *Ube3a-ATS*. Results are graphed as mean ± SEM from four biological replicates. $*P < 0.05$, $**P < 0.01$, $***P < 0.001$.

paternal allele was necessary for chromatin decondensation to occur, but did not identify a specific mechanism (28). The *Snord116* locus likely has a propensity for forming R loops because of the repeating units of GC skew, thus explaining the particular sensitivity of the region to inhibition of topoisomerase I by topotecan (12). We demonstrate that topotecan treatment results in increased R-loop formation within *Snord116* corresponding to increased chromatin decondensation and inhibition of transcriptional elongation through to *Ube3a-ATS* (Fig. 4*D*). Although the topotecan effects on R-loop levels observed by DRIP appear to show a smaller effect than those seen at the transcriptional levels, we hypothesize that the repetitive nature of the *Snord116* locus amplifies the effect of R loops individually forming at each repeat. These results predict that R-loop formation at the *Snord116* locus finely balances the chromatin state and transcription at the PWS/AS locus. Under physiologic conditions, R-loop formation and chromatin decondensation enable the transcription machinery to progress through to *Ube3a-ATS* to silence *Ube3a* in *cis*. However, under conditions that promote excess R-loop formation, such as topotecan treatment, R-loop formation and the resulting topological strain cause excessive stalling of the transcription machinery thereby preventing expression of *Ube3a-ATS* (Fig. 4*D*). The repetitive nature of the *Snord116* locus may contribute to the sensitivity of the region to topotecan because GC skew is present across the ∼100-kb *Snord116* repeat region (Fig. 3*A*). R-loop formation may also play a role in the physiologic regulation of *Ube3a-ATS* expression because R loops have been shown to form at the 3′ end of genes and contribute to transcription termination (24). Maintaining the optimal amount of R-loop formation and transcription in the locus will be important for therapies in AS or PWS that seek to alter transcription on the paternal or maternal allele to reverse the disease state.

Regulation of transcription termination in the *Snord116* region is part of normal neuron development because the *Snord116* region and *Ube3a-ATS* are expressed specifically in neurons, whereas *Snrpn* is expressed ubiquitously from the same promoter. Our finding that the *Snord116* region forms R loops in neurons under physiologic conditions, but that excessive R-loop formation terminates transcription, suggests that regulation of R-loop formation may be one mechanism by which transcription regulation occurs in the *Snrpn-Ube3a* locus. R loops have been shown to be part of transcription termination at the 3′ end of genes (24). Furthermore, inhibiting RNA processing events can lead to increased R-loop formation (33, 34). Although such a role underlies genomic instability, we hypothesize that regulation of alternative splicing and processing in the *Snord116* region could also modulate R-loop–mediated transcription termination in the locus.

UBE3A-ATS serves as an appealing target for therapy in AS because paternal *UBE3A* is intact in AS patients (35). The discovery of topoisomerase inhibitors as potential therapies for silencing *Ube3a-ATS* and activating paternal *UBE3A* is very promising (12), but concerns about toxicity and specificity remain (18). Our findings on the mechanism and site of action of topotecan in repressing paternal *Ube3a-ATS* may lead to refined strategies for reducing unwanted off-target effects of topoisomerase inhibitors in treating AS. We show that the *Snord116* locus is a critical region for mediating the effects of topoisomerase inhibition on *Ube3a-ATS* expression. Because inhibiting RNA processing can increase R-loop formation (33, 34), one strategy may be to target splicing and RNA processing of the *Snord116* and *116HG* transcript to inhibit transcription leading to *Ube3a-ATS*.

Materials and Methods

NPC and Neuron Culture. B6(Cg)-Snord116$^{tm1.1Uta}$/J (*Snord116del*) mice were obtained from Jackson Labs, housed in a 24-h light/dark cycle, temperature-controlled room, and fed a standard diet of Picolab mouse chow 20 (PMI International). NPCs were isolated from E15.5 mouse brain (36) and grown in NEP Complete media without serum supplemented glutamax. For differentiation, media was changed to NEP Basal with retinoic acid, and 50% of media was replaced every 3.5 d. For topotecan treatment of neurons, after 7 d in vitro, 300 nM topotecan (Sigma) was added, and neurons were grown for 3 more days.

Episome and Plasmid Construct. Genomic DNA was PCR amplified and ligated into the pGEM-T vector (Promega). Sequence-confirmed inserts were subsequently cloned between CMV-TetOn promoter and IRES-GFP sequences. *mAirn* G-skew and C-skew sequences were characterized (23). The mouse *Snord116* episome carries a single 1,050-bp fragment most closely matching chr7:67,007,613–67,008,662 (mm9, 97% identity). The human *Snord116* episome carries a single 1,087-bp fragment matching chr15:25,299,483–25,300,569 (hg19).

Episome Culture. HEK-293 cells stably maintaining episomes were grown in selective media (200 μg/mL Hygromycin) and treated with 1 μg/mL doxycycline to induce transcription. RNA or chromatin was harvested 48 h later.

RNA Extraction. RNA was extracted from neurons using manufacturer's protocol for RNeasy mini kit (Qiagen).

DNA FISH. DNA FISH was performed as described (28).

RNA FISH. Cells grown on coverslips were fixed in Histochoice for 15 min, washed in 1× PBS, and stored in 70% (vol/vol) EtOH at −20 °C. Slides were dehydrated in 100% EtOH and probe resuspended in SureFISH hybridization buffer (Agilent) was applied. Hybridization was performed overnight at 37 °C before washing coverslips twice in 2× SSC/0.1% IGEPAL at 37 °C and mounting in SureFISH mounting buffer (Agilent) with DAPI at 5 μg/mL using novel custom probes for *Ube3a*, as well as *115HG* and *116HG* probes, described previously (11).

Microscopy. Microscopy was performed as described (28). Two individuals blind to the conditions analyzed DNA FISH and RNA FISH slide. For RNA FISH, four biological replicates (150–200 nuclei per replicate) were analyzed. For DNA FISH, two biological replicates (40 nuclei per replicate) were analyzed. Two-tailed Student's *T* test was performed to test for significance.

qRT-PCR and qPCR. qRT-PCR and qPCR were performed as described (37) with custom primers listed in Table S1. Two-tailed Mann–Whitney *u* test was used to test for statistical significance of qRT-PCR. RNA was analyzed from six biological replicates.

For GC skew maps, GC skew was generated using a custom Perl script to calculate within a 500-bp window the G-skew defined as $((G - C)/(G + C))$.

Immunostaining. Immunostaining for RNA:DNA hybrids was performed as described (28) using the S9.6 antibody (23). For RNase H treatment of slides, after postfixation, slides were incubated in 1× RNase H buffer with 10 units of RNase H (NEB).

Immuno-FISH. For immuno-FISH slides were prepared as for immunostaining above. After staining, slides were washed in 1xPBS/0.2% tween, fixed in 1% formaldehyde, and washed three times in 1× PBS. Slides were dehydrated in a series of 50%/70%/90%/100% EtOH washes, and hybridization was performed as for DNA FISH.

DRIP. For DRIP, genomic DNA (gDNA) was extracted from cultured neurons as described (23). gDNA was extracted from one hemisphere of a mouse cerebellum by homogenizing in 1× PBS, and nuclei were pelleted and resuspended in R-loop lysis buffer. Episomal DNA was extracted by resuspending cells in 10 mM EDTA/10 mM Tris·Cl (pH 7.5) before lysing cells with 0.5% SDS and pelleting gDNA with 1.25 M NaCl at 4 °C overnight. gDNA and Episomal DNA was digested with HinDIII, EcoRI, SspI, BsrGI, and XbaI. DRIP was performed as described (23) with 8 μg of DNA and 10 μg of antibody. DRIP on topotecan treated neurons was performed on four biological replicates and two-tailed Mann–Whitney *u* test was used for statistical testing. Cerebellum DRIP was performed on three biological replicate samples, and two-tailed Student *t* test was used for significance testing.

ChIP. Chromatin immunoprecipitation was performed as described (37) using an antibody for total histone H3 (Abcam ab1791) or RNA PolII 8WG16 (Abcam ab817). Brain and liver nucleosome occupancy was compared from three animals and two-tailed Student *t* test was used for significance testing. Pol-II ChIP was performed on three biological replicates. Episome DRIP and ChIP was performed on six biological replicates and two tailed Mann–Whitney *u* test was used for significance testing.

IVT R-Loop Gel Shift. Plasmids were in vitro transcribed with T7, Sp6, or T3 RNA polymerase (Promega) for 30 min and heat inactivated at 65 °C for 5 min. Sample was treated with RNase H (NEB) or mock treated. DNA was precipitated with ethanol and washed before agarose gel electrophoresis stained with Sybr Gold (Invitrogen).

Dot Blot R-Loop Assay. Plasmids were in vitro transcribed as for the gel-shift assay. Purified plasma DNA (250 ng) was blotted on a membrane and cross-linked to the membrane with UV. The membrane was blocked with Odyssey blocking buffer (Odyssey) for 30 min, and incubated with 5 μg of S9.6 antibody. Blots were washed in 1× PBS/0.2% Tween-20, and DAMIG-800 in blocking buffer (Odyssey) was added at room temperature for 2 h. The membrane was washed with 1× PBS/0.2% Tween and scanned on a Licor Odyssey scanner.

ACKNOWLEDGMENTS. We thank David Segal for critical reading of the manuscript and Diane Schroeder for helpful discussions. This work funded was by Grants National Institutes of Health (NIH) F31NS073164 (to W.T.P.), NIH 1R01NS076263 (to J.M.L.), and NIH 1R01GM094299 (to F.C.) and the Prader–Willi Foundation.

1. Chamberlain SJ, Lalande M (2010) Angelman syndrome, a genomic imprinting disorder of the brain. *J Neurosci* 30(30):9958–9963.
2. Cassidy SB, Schwartz S, Miller JL, Driscoll DJ (2012) Prader-Willi syndrome. *Genet Med* 14(1):10–26.
3. Kishino T, Lalande M, Wagstaff J (1997) UBE3A/E6-AP mutations cause Angelman syndrome. *Nat Genet* 15(1):70–73.
4. Matsuura T, et al. (1997) De novo truncating mutations in E6-AP ubiquitin-protein ligase gene (UBE3A) in Angelman syndrome. *Nat Genet* 15(1):74–77.
5. Sahoo T, et al. (2008) Prader-Willi phenotype caused by paternal deficiency for the HBII-85 C/D box small nucleolar RNA cluster. *Nat Genet* 40(6):719–721.
6. de Smith AJ, et al. (2009) A deletion of the HBII-85 class of small nucleolar RNAs (snoRNAs) is associated with hyperphagia, obesity and hypogonadism. *Hum Mol Genet* 18(17):3257–3265.
7. Duker AL, et al. (2010) Paternally inherited microdeletion at 15q11.2 confirms a significant role for the SNORD116 C/D box snoRNA cluster in Prader-Willi syndrome. *Eur J Hum Genet* 18(11):1196–1201.
8. Skryabin BV, et al. (2007) Deletion of the MBII-85 snoRNA gene cluster in mice results in postnatal growth retardation. *PLoS Genet* 3(12):e235.
9. Ding F, et al. (2008) SnoRNA Snord116 (Pwcr1/MBII-85) deletion causes growth deficiency and hyperphagia in mice. *PLoS One* 3(3):e1709.
10. Vitali P, Royo H, Marty V, Bortolin-Cavaillé ML, Cavaillé J (2010) Long nuclear-retained non-coding RNAs and allele-specific higher-order chromatin organization at imprinted snoRNA gene arrays. *J Cell Sci* 123(Pt 1):70–83.
11. Powell WT, et al. (2013) A Prader-Willi locus lncRNA cloud modulates diurnal genes and energy expenditure. *Hum Mol Genet*, 10.1093/hmg/ddt281.
12. Huang HS, et al. (2012) Topoisomerase inhibitors unsilence the dormant allele of Ube3a in neurons. *Nature* 481(7380):185–189.
13. Runte M, et al. (2001) The IC-SNURF-SNRPN transcript serves as a host for multiple small nucleolar RNA species and as an antisense RNA for UBE3A. *Hum Mol Genet* 10(23):2687–2700.
14. Meng L, Person RE, Beaudet AL (2012) Ube3a-ATS is an atypical RNA polymerase II transcript that represses the paternal expression of Ube3a. *Hum Mol Genet* 21(13):3001–3012.
15. Latos PA, et al. (2012) Airn transcriptional overlap, but not its lncRNA products, induces imprinted Igf2r silencing. *Science* 338(6113):1469–1472.
16. Le Meur E, et al. (2005) Dynamic developmental regulation of the large non-coding RNA associated with the mouse 7C imprinted chromosomal region. *Dev Biol* 286(2):587–600.
17. Landers M, et al. (2004) Regulation of the large (approximately 1000 kb) imprinted murine Ube3a antisense transcript by alternative exons upstream of Snurf/Snrpn. *Nucleic Acids Res* 32(11):3480–3492.
18. Beaudet AL (2012) Angelman syndrome: Drugs to awaken a paternal gene. *Nature* 481(7380):150–152.
19. Staker BL, et al. (2002) The mechanism of topoisomerase I poisoning by a camptothecin analog. *Proc Natl Acad Sci USA* 99(24):15387–15392.
20. Liu LF, Wang JC (1987) Supercoiling of the DNA template during transcription. *Proc Natl Acad Sci USA* 84(20):7024–7027.
21. French SL, et al. (2011) Distinguishing the roles of Topoisomerases I and II in relief of transcription-induced torsional stress in yeast rRNA genes. *Mol Cell Biol* 31(3):482–494.
22. El Hage A, French SL, Beyer AL, Tollervey D (2010) Loss of Topoisomerase I leads to R-loop-mediated transcriptional blocks during ribosomal RNA synthesis. *Genes Dev* 24(14):1546–1558.
23. Ginno PA, Lott PL, Christensen HC, Korf I, Chédin F (2012) R-loop formation is a distinctive characteristic of unmethylated human CpG island promoters. *Mol Cell* 45(6):814–825.
24. Skourti-Stathaki K, Proudfoot NJ, Gromak N (2011) Human senataxin resolves RNA/DNA hybrids formed at transcriptional pause sites to promote Xrn2-dependent termination. *Mol Cell* 42(6):794–805.
25. Aguilera A, García-Muse T (2012) R loops: From transcription byproducts to threats to genome stability. *Mol Cell* 46(2):115–124.
26. Belotserkovskii BP, Hanawalt PC (2011) Anchoring nascent RNA to the DNA template could interfere with transcription. *Biophys J* 100(3):675–684.
27. Belotserkovskii BP, et al. (2010) Mechanisms and implications of transcription blockage by guanine-rich DNA sequences. *Proc Natl Acad Sci USA* 107(29):12816–12821.
28. Leung KN, Vallero RO, DuBose AJ, Resnick JL, LaSalle JM (2009) Imprinting regulates mammalian snoRNA-encoding chromatin decondensation and neuronal nucleolar size. *Hum Mol Genet* 18(22):4227–4238.
29. Hung SH, Yu Q, Gray DM, Ratliff RL (1994) Evidence from CD spectra that d(purine).r(pyrimidine) and r(purine).d(pyrimidine) hybrids are in different structural classes. *Nucleic Acids Res* 22(20):4326–4334.
30. Dunn K, Griffith JD (1980) The presence of RNA in a double helix inhibits its interaction with histone protein. *Nucleic Acids Res* 8(3):555–566.
31. Tuduri S, et al. (2009) Topoisomerase I suppresses genomic instability by preventing interference between replication and transcription. *Nat Cell Biol* 11(11):1315–1324.
32. Kuehner JN, Pearson EL, Moore C (2011) Unravelling the means to an end: RNA polymerase II transcription termination. *Nat Rev Mol Cell Biol* 12(5):283–294.
33. Stirling PC, et al. (2012) R-loop-mediated genome instability in mRNA cleavage and polyadenylation mutants. *Genes Dev* 26(2):163–175.
34. Li X, Manley JL (2005) Inactivation of the SR protein splicing factor ASF/SF2 results in genomic instability. *Cell* 122(3):365–378.
35. Mabb AM, Judson MC, Zylka MJ, Philpot BD (2011) Angelman syndrome: Insights into genomic imprinting and neurodevelopmental phenotypes. *Trends Neurosci* 34(6):293–303.
36. Hutton SR, Pevny LH (2008) Isolation, culture, and differentiation of progenitor cells from the central nervous system. *Cold Spring Harb Protoc*, 10.1101/pdb.prot5077.
37. Gonzales ML, Adams S, Dunaway KW, LaSalle JM (2012) Phosphorylation of distinct sites in MeCP2 modifies cofactor associations and the dynamics of transcriptional regulation. *Mol Cell Biol* 32(14):2894–2903.